

The sustainability of water resources in the High Mountain Asia in the context of recent and future glacier change

Ann V. Rowan^{1*}, Duncan J. Quincey², Morgan J. Gibson³, Neil F. Glasser³, Matthew J. Westoby⁴, Tristram D.L. Irvine-Fynn³, Phillip R. Porter⁵, Michael J. Hambrey³

¹*Department of Geography, University of Sheffield, Winter Street, Sheffield, S10 2TN, UK*

*Corresponding author; email: a.rowan@sheffield.ac.uk

²*School of Geography, University of Leeds, LS2 9JT, UK*

³*Centre for Glaciology, Department of Geography and Earth Sciences, Aberystwyth University, SY23 3DB, UK*

⁴*School of Engineering and Environment, Northumbria University, Newcastle upon Tyne, NE1 8ST*

⁵*University of Hertfordshire, Hatfield, Hertfordshire. AL10 9AB, UK*

Abstract

High Mountain Asia contains the largest volume of glacier ice outside the Polar regions, and contain the headwaters of some of the largest rivers in central Asia. These glaciers are losing mass at a mean rate of between -0.18 ± 0.04 m and -0.5 m water equivalent per year. While glaciers in the Himalaya are generally shrinking, those in the Karakoram have experienced a slight mass gain. Both changes have occurred in response to rising air temperatures due to Northern Hemisphere climatic change. In the Westerly influenced Indus catchment, glacier meltwater makes up a large proportion of the hydrological budget, and loss of glacier mass will ultimately lead to a decrease in water supplies. In the monsoon-influenced Ganges and Brahmaputra catchments, the contribution of glacial meltwater is relatively small compared to the Indus, and the decrease in annual water supplies will be less dramatic. Therefore, enhanced glacier melt will increase river flows until the middle of the 21st Century, but in the longer-term into the latter part of this century, river flows will decline as glaciers shrink. Declining meltwater supplies may be compensated by increases in precipitation, but this could exacerbate the risk of flooding.

1. Introduction

Millions of people rely on glaciers in the Himalaya, Karakoram and Hindu Kush mountains, collectively referred to as High Mountain Asia, as a water resource. These glaciers form the headwaters of the largest rivers in Asia, including the Indus, the Ganges and the Brahmaputra Rivers (Fig. 1) and as such the mountains are often referred to as the ‘water towers of Asia’ (Immerzeel *et al.* 2010). High Mountain Asia contains the largest glacierised area outside the

39 Polar regions (Bolch *et al.* 2012) and glaciers here are highly sensitive to climate change
40 (Solomina *et al.* 2016). Glaciers in the Himalaya are predominantly shrinking (Kääb *et al.*
41 2012), and rates of glacier mass loss, although spatially variable, have accelerated since the
42 1990s (Bolch *et al.* 2012). If a constant rate of glacier mass loss after 1975 is assumed, then
43 predictions indicate loss of 10–30 m water equivalent (w.e.) per year between 2010 and 2035,
44 which is sufficient to result in the disappearance of many smaller glaciers across the
45 mountain range (Cogley 2011). The catchments supplied by rivers draining High Mountain
46 Asia are located in developing countries that use this water primarily for agriculture and
47 hydroelectric power generation, and are extremely vulnerable to changes in their water
48 supply (Kaser *et al.* 2010; Pritchard, 2017). Predictions are needed of how Asian water
49 supplies are likely to change due to continued glacier mass loss in response to recent and
50 future climate change. We therefore need to improve understanding of both the contribution
51 of glaciers to the hydrological budgets of these large catchments, and discover how these
52 glaciers are responding to recent and future climate change (e.g. Lutz *et al.* 2014; Brun *et al.*
53 2017).

54

55 Although only 1–3% of the area of the Indus, Ganges and Brahmaputra catchments are
56 glacierised, these densely-populated catchments rely on glacial meltwater (Immerzeel *et al.*
57 2010). The contribution of glaciers to runoff varies regionally; from 18.8% in the Dudh
58 Koshi catchment, which is a major tributary of the Ganges, up to 80.6% in the Hunza
59 catchment that drains into the Indus (Lutz *et al.* 2014). The Indus and the Ganges provide
60 important water supplies that are used to irrigate over 140,000 km² of agricultural land, and
61 the largest irrigation network in the world is contained in the Indus catchment (Immerzeel *et al.*
62 2010). In particular, the importance of glacier meltwater relative to other water sources
63 (e.g. precipitation, snow melt, groundwater) for regional hydrological budgets has only
64 recently been documented (Immerzeel *et al.* 2010, Lutz *et al.* 2014). In the monsoon-
65 influenced Central and Eastern Himalaya the majority of annual precipitation occurs during
66 the warm summer monsoon months (June to September) (Bookhagen & Burbank 2010). The
67 high summer rainfall and snowfall roughly coincide with the timing of the majority of glacier
68 ablation (Benn & Lehmkuhl 2000), so that the relative contribution of glacial melt to river
69 flows is minimised compared to regions to the west where summers are generally dry (Kaser
70 *et al.* 2010). In the Western Himalaya, Karakoram and Hindu Kush mountains, where the
71 majority of precipitation occurs as winter snowfall, glacier melt plays a much more important
72 role in regulating seasonal river flows, with a relatively larger proportion of the annual flow
73 in the Indus resulting directly from glacier melt compared to that in the Ganges and
74 Brahmaputra catchments (Lutz *et al.* 2014).

75

76 The impact of climate change on these vital river flows from the Himalaya is, however, not
77 straightforward. For example, climatic warming may cause glaciers to lose mass and release a
78 greater volume of meltwater each year, but may also result in increased orographic
79 precipitation that could sustain or enhance flows and trigger a gradual or abrupt change in the
80 seasonality of peak flows (Immerzeel *et al.* 2010). Understanding regional and catchment-
81 scale hydrological budgets and predicting how they will vary under a changing climate
82 therefore requires coupling our understanding of glaciers processes with climate model
83 forecasts. The Intergovernmental Panel on Climate Change (IPCC) climate scenarios for the
84 21st Century are used for this purpose, as they are compiled from comparison of an ensemble
85 of state-of-the-art climate model outputs (Collins *et al.* 2013). Many regional hydrological
86 models contain large uncertainties as they do not capture the processes that affect individual
87 glaciers, and so detailed catchment-scale models validated by field data are also required to
88 better constrain future hydrological changes (e.g. Ragetli *et al.* 2016).

89

90 Here we review recent and predicted glacier and hydrological change across High Mountain
91 Asia (Fig. 1). Glaciers on the Tibetan Plateau are excluded from this review, as this region is
92 strongly influenced by weather systems originating from the Arctic rather than the Asian
93 monsoon, and show markedly different behaviour compared to these glaciers. The long-term
94 response to climate change of Tibetan glaciers is described by Owen *et al.* (2008) and Owen
95 (2009). We first summarise the current knowledge of the state of glaciers in High Mountain
96 Asia, then discuss these changes in the context of observed longer-term glacier change since
97 the late Holocene (the last 2,000 years). We then compare predictions of glacier change with
98 current and future climate change and consider the likely impacts of these changes on
99 regional hydrological budgets.

100

101 **2. The current state of glaciers in High Mountain Asia**

102 Glaciers in High Mountain Asia are discussed in terms of their location in sub-regional areas
103 that are defined from the major regional climate controls (after Bolch *et al.* 2012; Fig. 1).
104 From east to west these regions are: the monsoon-influenced Eastern and Central Himalaya,
105 and the mid-latitude Western Himalaya, Karakoram and Hindu Kush ranges influenced by
106 westerly weather systems. These areas follow the boundaries of the major river catchments
107 within the high mountains, with the Western Himalaya, Karakoram and Hindu Kush draining
108 into the Indus, the Central Himalaya into the Ganges, and the Eastern Himalaya and some of
109 the Tibetan Plateau forming the headwaters of the Brahmaputra River.

110

111 **2.1 Glacier extent and volume**

112 The Himalaya and Karakoram mountains contain 32,353 glaciers with a total glacierised area
113 of about 41,000 km² equivalent to 6% of the global glacierised area (Arendt *et al.* 2015).

114 Until recently, relatively little was known about the total number and size of glaciers in the
115 Himalaya because perennial snow cover, debris-covered ice and ice-cored moraine impeded
116 identification of glacier outlines from satellite observations. Improvements in satellite remote
117 sensing imagery have allowed identification of the majority of glacier outlines, which are
118 compiled in the 6th Randolph Glacier Inventory (released in July 2017) and cover most of
119 High Mountain Asia (Arendt *et al.* 2015). Global glacier inventories comprising glacier area
120 boundaries drawn by the glaciological community are now sufficiently complete to estimate
121 the glacierised extents, but data describing other important characteristics such as ice
122 thickness are highly spatially variable and are limited by the small number of field
123 observations. Glacier volume is more difficult to measure than area, as ice thickness is also
124 unknown for most of the range. Estimated mean ice thickness for all glaciers in the Global
125 Land Ice Measurements from Space database are low compared to typical values from
126 individual glaciers derived from field data. Mean ice thickness is estimated to be 86 m for the
127 Himalaya, and 172 m for the Karakoram (<http://glims.colorado.edu/glacierdata/> accessed on
128 30/09/16), although the uncertainty associated with these values is undoubtedly large (Cogley
129 2011; Frey *et al.* 2014) and likely biased by the majority of measurements being obtained
130 from smaller glaciers.

131

132 More robust *in situ* ice thickness measurements have only been made for a handful of
133 glaciers, using ground-penetrating radar or radio-echo sounding surveys. Access to large
134 high-altitude glaciers can be challenging and so field observations are frequently made at
135 more accessible glaciers. Accessible glaciers are generally at lower altitudes, smaller than the
136 majority of the population, and have higher rates of mass loss than larger glaciers at higher
137 altitude. These glaciers are not necessarily representative of regional-scale behaviour, and
138 therefore field measurements often contain a bias that may skew understanding of regional
139 mass balance trends (Fujita & Nuimura 2011). Ice thicknesses for three glaciers in Nepal in
140 the Central Himalaya ranged from less than 20 m near the terminus to 440 m near the icefall for
141 the largest, Khumbu Glacier (glacier area is 39.5 km²; Gades *et al.* 2000), 20–157 m for
142 Lirung Glacier (13.5 km²; Kadota *et al.* 1997) to 51–86 m for the smallest, Glacier AX010
143 (0.6 km²; Kadota *et al.* 1997). Ice thickness was 124–270 m for Chhota Shigri Glacier (15.7
144 km²) in the Western Himalaya (Azam *et al.* 2012). These values represent the centreline ice
145 thickness, and in each case the glacier cross-section thins towards the valley sides (*cf.* Azam
146 *et al.* 2012).

147

148 Across the Himalaya, 14–18% of the glacierised area is debris covered (Kääb *et al.* 2012), the
149 extent of which increases to the east to reach 36% in the Everest region of Nepal (Thakuri *et al.*
150 *et al.* 2014). Supraglacial debris thickness typically increases down-glacier, as englacial and
151 supraglacial debris transport concentrates sediment previously incorporated into the ice (Fig.

152 2) (Rowan *et al.* 2015). The thickness of supraglacial debris layers can exceed several metres
153 (Nicholson & Benn 2013, Thakuri *et al.* 2014; Soncini *et al.* 2016). Supraglacial debris
154 modifies glacier mass balance, either through enhancing ablation due to the decreased albedo
155 of debris compared to ice, or by reducing ablation by insulating the glacier surface; feedbacks
156 which are largely dependent on the thickness of the debris layer (Østrem 1959, Evatt *et al.*
157 2015, Nicholson & Benn 2006). The threshold between the enhancement or attenuation of
158 ablation by supraglacial debris occurs at a critical thickness of around 0.05 m, as
159 demonstrated both from field (Rounce *et al.* 2015) and laboratory measurements
160 (Reznichenko *et al.* 2010). The influence of variations in debris thickness on ablation was
161 demonstrated at Khumbu Glacier, where rates of surface lowering are highest mid-glacier just
162 below the icefall where the surface is either debris free or only thinly mantled compared to
163 the heavily debris-mantled terminus where ablation rates are an order of magnitude lower
164 (Nakawo *et al.* 1999, Adhikari & Huybrechts 2009, Owen *et al.* 2009).

165

166 **2.2 State of glacier mass balance and their Equilibrium Line Altitudes**

167 Glacier mass balance is highly variable across High Mountain Asia. This variability in mass
168 balance has been identified directly using the traditional glaciological method where stakes
169 are inserted into the glacier surface to measure ice ablation and snow accumulation (e.g.
170 Soncini *et al.* 2016). Equilibrium Line Altitude (ELA; the point on a glacier at which
171 accumulation and ablation are balanced) can be estimated from the areal extent and
172 hypsometry combined with climate data (Benn & Lehmkuhl 2000). The ELA method has the
173 advantage of allowing reconstructions of past glacier mass balance from geological evidence
174 of glacier extent (Benn *et al.* 2005, Owen & Benn 2005). Regional glacier mass balance can
175 be estimated from geodetic methods using multi-temporal satellite imagery that measures
176 changes in glacier surface elevations (e.g. Bolch *et al.* 2011, Kääb *et al.* 2012). Remote
177 sensing can also be used to measure snowline altitudes at the end of the ablation season, from
178 which the ELA can be derived (e.g. Harper & Humphrey 2003). Mass balance is more
179 difficult to measure for debris-covered glaciers than for clean-ice glaciers due to the rapid
180 variations in rates of ablation that occur across the glacier surface, influenced by the thermal
181 conductivity of the debris layer, which is controlled by factors including debris thickness,
182 debris grain size, porosity and water content (Benn *et al.* 2012).

183

184 Mass balance has only been measured directly for a small number of glaciers (Fig. 3), and the
185 longest of the continuous records cover only 10 years. Mass balance for Shaune Garang
186 Glacier in the Himachal Pradesh in northern India was $-0.36 \text{ m w.e. a}^{-1}$ between 1981 and
187 1991 (Pratap *et al.* 2015). Measurements of mass balance for small glaciers in the Central
188 Himalaya indicate the extreme sensitivity of the monsoon-influenced glaciers to air
189 temperature. Mass balance measurements through the 1978 monsoon for Glacier AX010

190 indicate that a 0.5°C decrease in mean summer air temperature would result in a transition
191 between positive and negative mass balance (Ageta *et al.* 1980). Three annual ablation stake
192 surveys indicate a mass balance of $-1.6 \text{ m w.e. a}^{-1}$ between 2003 and 2014 for Gangju La
193 Glacier, a small clean-ice glacier in Bhutan in the Eastern Himalaya (Tshering & Fujita
194 2016). Mass balance modelling for the partially debris-covered Langtang Glacier in the
195 Central Himalaya simulated a mass balance of $-0.11 \text{ m w.e. a}^{-1}$ between 1987 and 1997
196 (Sharma & Owen 1996). Mean present-day ELA calculated from snowline elevations in the
197 Annapurna region of western Nepal was $\sim 5050 \text{ m}$ (Harper & Humphrey 2003) and in eastern
198 Nepal the ELA ranged from 5300 m in the Langtang Valley to 5600 m in the Khumbu Valley
199 (Kayastha & Harrison 2008).

200

201 The complete mass budget of all glaciers in High Mountain Asia between 2000 and 2016 was
202 recently calculated from remote topographic measurements as $-0.18 \pm 0.04 \text{ m w.e. a}^{-1}$ (Brun
203 *et al.* 2017). This value is slightly lower than that given by glaciological mass balance records
204 (summarised by Bolch *et al.* 2012) which gave a regional mass budget of about $-0.3 \text{ m w.e. a}^{-1}$
205 ¹ between the 1960s and 1990s, becoming increasingly more negative during the last two
206 decades and similar to the global mean (around $-0.5 \text{ m w.e. a}^{-1}$). Remote sensing studies have
207 previously indicated a slightly more negative regional mass balance between 2003 and 2008
208 of $-0.21 \pm 0.05 \text{ m w.e. a}^{-1}$, lower than the global average due to the slightly positive mass
209 budget in the Karakoram (Kääb *et al.* 2012)—the so-called ‘Karakoram anomaly’ (Gardelle
210 *et al.* 2012). Karakoram glaciers have recently gained mass due to rising air temperatures
211 delivering more winter snowfall from the Arabian Gulf (Kapnick *et al.* 2014). A large
212 proportion of surge-type glaciers are found in the Karakoram, and this dynamic behavior can
213 also result in short-term mass gain (Quincey *et al.* 2011; Quincey *et al.* 2015).

214

215 **2.3 The “debris-cover anomaly”**

216 The ablation areas of many glaciers in the Himalaya are covered with rock debris, which is
217 deposited on glacier surfaces as a result of erosion and mass wasting of the surrounding
218 landscape. Supraglacial debris affects mass balance and complicates understanding of the
219 response of these debris-covered glaciers to climate change (Scherler *et al.* 2011). There are
220 four main sources of debris on the surface of Himalayan glaciers: (1) rockfall debris which is
221 angular in character; (2) mixed rock- and ice-avalanche debris, which is texturally similar,
222 but which is entrained as prominent debris layers within the glacier (Fig. 2d); (3) material
223 resulting from collapse from over-steepened moraines which is characterised by sandy
224 boulder gravel and is typically sub-rounded to angular; (4) debris derived from the base of the
225 glacier that has been transported to the surface by thrusting or shear from the bed, such as at
226 the base of an icefall. This debris is a mixture of silt, sand and gravel, with some boulders
227 bearing striations. These four lithofacies become intimately mixed on the surface of debris-

228 covered glaciers due to local slope movements from uneven ablation (Figure 2c) (Hambrey *et*
229 *al.* 2008). Many Himalayan glaciers are also bounded by prominent latero-terminal moraine
230 systems. These moraines are comprised of a mixture of basally worked and rockfall debris,
231 which texturally are typically sandy boulder-gravels. Downwasting of the glaciers since the
232 Little Ice Age (LIA) about 1300–1600 (Rowan, 2017) have left ice-cored moraines up to a
233 hundred metres above the glacier surface, which result in an unstable inner moraine face that
234 is unstable and prone to collapse (Hambrey *et al.* 2008).

235

236 Debris-covered Himalayan glaciers tend to lose mass by surface lowering rather than
237 terminus recession (Rowan *et al.* 2015, Quincey *et al.* 2009, Bolch *et al.* 2011). Surface
238 lowering causes these debris-covered glaciers to develop very low or even reversed long-
239 profile topographic gradients through their ablation areas, which promotes the formation of
240 supraglacial water bodies. These ponds and lakes influence the seasonal transport of water
241 through the glacial system, and can expand and coalesce to form substantial supraglacial or
242 proglacial, moraine-dammed lakes that may eventually pose a potential flood hazard (Watson
243 *et al.* 2016, Thompson *et al.* 2012). Such features are commonly bordered by steep, debris-
244 free ice cliffs, which progressively backwaste, and, if connected to a supraglacial pond or
245 lake, may undergo thermoerosional notch development at the ice-water interface, promoting
246 the onset of calving processes (Fig. 2) (Hambrey *et al.* 2008, Thompson *et al.* 2016).

247

248 Satellite observations of glacier mass change suggest that debris-covered glaciers in the
249 Himalaya and Karakoram may be losing mass at the same rate as those glaciers with clean-
250 ice (debris-free) surfaces. This ‘debris-cover anomaly’ could be due to enhancement of
251 ablation at ice cliff faces. Although the exposure of clean ice at these ice cliffs can
252 dramatically enhance local ablation rates (Miles *et al.* 2016, Brun *et al.* 2016, Reid & Brock
253 2014) field observations from Changri Nup Glacier in the Everest region suggest that, despite
254 the presence of these ablation ‘hotspots’, a continuous or near-continuous mantle of
255 supraglacial debris reduces net ablation, such that glacier-wide mass loss is less than would
256 be the case for an equivalent clean-ice glacier (Vincent *et al.* 2016). To fully understand the
257 effect of ice cliffs on ablation from debris-covered glaciers, these features and their evolution
258 need to be incorporated into glacier-wide surface energy balance modelling (e.g. Buri *et al.*
259 2016; Brun *et al.* 2016).

260

261

262 **3. Changes in glacier volume during the Late Holocene**

263 Changes in the areal extent and volume of glaciers over the last 2,000 years can be inferred
264 from moraines that indicate the position of glacier margins, historical observations made by
265 climbing expeditions, and field and satellite measurements of glacier geometries.

266

267 ***3.1 Late Holocene (2,000 years ago to present)***

268 Many glaciers in High Mountain Asia have advanced and receded two or three times during
269 the last 2,000 years in response to climate change (Owen & Dortch 2014, Murari *et al.* 2014,
270 Rowan 2017) and followed the global trend of glacier recession and shrinkage since about
271 1850 (Thompson *et al.* 2006). The last period of regional glacier advance was the LIA which
272 peaked between 1300 and 1600, although glaciers remained close to their LIA limits until the
273 20th Century (Rowan 2017). These observations are based on geochronological data for
274 moraines compiled from studies using radiocarbon (¹⁴C) dating (e.g. Muller 1961,
275 Röthlisberger & Geyh 1986) and terrestrial cosmogenic nuclide dating (e.g. Owen 2009,
276 Murari *et al.* 2014). More recent applications of these techniques generally provide more
277 accurate results due to improvements in laboratory measurement protocols. Regional glacier
278 volume change in the Himalaya over decadal to centennial timescales occurred in response to
279 hemispheric changes in air temperature (Solomina *et al.* 2016, Rowan 2017). However,
280 variations in the timing and extent of glacier volume change across this range are primarily
281 driven by millennial-scale east–west and north–south variations in atmospheric circulation
282 regimes (Vaux & Balk 2012). The characteristics of local weather systems, particularly
283 precipitation distribution, are also important and probably governed by precession-scale
284 insolation cycles (Thompson *et al.* 2006). Consequently, moraine ages indicate spatial
285 variability in the amount and timing of glacier mass loss due to variations in the timing and
286 intensity of monsoonal and Westerly snowfall across the region (Rowan 2017, Owen 2009).

287

288 ***3.2 20th and 21st Centuries (1900 to present)***

289 Changes in glacier length and area during the early part of the 20th Century are described by
290 historical accounts from early climbing expeditions. These records are based on visual
291 comparison of the state of these glaciers to those in the European Alps, which has led to
292 misinterpretation of ongoing glacier volume change (Grove 2004). Measurements of changes
293 in length and area are of limited use for estimating the mass change of debris-covered
294 glaciers that lose mass by surface lowering rather than terminus recession (e.g. Bolch *et al.*
295 2011). Geochronological techniques such as ¹⁴C and terrestrial cosmogenic nuclide dating do
296 not currently operate at sufficient temporal resolution to describe the ages of moraines
297 formed in the last 100 years. However, changes in glacier volume over small areas can be
298 accurately detected by comparing multi-temporal aerial and satellite topographic data,

299 including historical imagery from the Corona and HEXAGON satellites that date back to the
300 1950s (e.g. Bolch *et al.* 2011; Berthier *et al.* 2014). Measurements of the gravitational field of
301 the Earth's surface (the Gravity Recovery and Climate Experiment; GRACE; Tapley *et al.*
302 2004) combined with topographic data can be used to estimate changes in glacier mass across
303 a broad spatial area (e.g. Ageta *et al.* 1980, Fujita & Nuimura 2011, Sarikaya *et al.* 2012) but
304 with large uncertainties (Gardner *et al.* 2013).

305

306 Analyses of ice cores demonstrate a sharp decrease in accumulation on low-latitude (25–
307 35°N) Himalayan glaciers, and an increase in ice volume at higher latitudes (35–70°N) on the
308 Tibetan Plateau driven by variability in monsoon intensity and timing since 1950 (Hou *et al.*
309 2002). However, glacier mass loss at high elevations has exceeded that which could be
310 attributed to change in monsoon intensity alone (Mölg *et al.* 2012). Mass balance is most
311 negative in the Eastern Himalaya, and becomes less negative to the north and in the northern
312 and eastern parts of the Karakoram where some glaciers showed slightly positive mass
313 balances between 1999 and 2008 (Gardelle *et al.* 2012). The opposing trends in glacier mass
314 balance between the Karakoram and the Eastern Himalaya over the last 50 years are
315 attributed to spatial variations in the rates of change in temperature and precipitation
316 (Gardelle *et al.* 2012, Nakawo *et al.* 1999), as rising Northern Hemisphere air temperatures
317 deliver winter snowfall from the Arabian Gulf further into the range (Kapnick *et al.* 2014).
318 Climate warming appears to have accelerated the mass loss from glaciers in the Himalaya
319 after 1995, reflecting the high sensitivity of the regional energy balance to small changes in
320 climate (Cogley 2011). Over the same period, a slight gain in mass has been observed for
321 glaciers in the Karakoram, attributed to a greater influence of Westerly winter snowfall
322 (Gardelle *et al.* 2012, Yao *et al.* 2012), although not all glaciers in the Karakoram gained
323 mass in the last 40 years (Sarikaya *et al.* 2012).

324

325 **4. Predictions of future glacier change**

326 Predictions of how glaciers will continue to change from the present day requires
327 quantifying, specifically: current glacier mass balances, the response time over which glaciers
328 will reach equilibrium with climate, and how the climate will change over the period of
329 interest. For the 21st and 22nd Centuries, climate model ensembles such as those produced by
330 the IPCC (Collins *et al.* 2013) give a range of possible warming values for future emissions
331 scenarios, which are useful for forcing meteorological and glacier modelling. Glacier models
332 are often somewhat less sophisticated than these climate models and operate at different
333 spatial scales, particularly in representing the dynamics of mountain glaciers, in which the
334 processes controlling the flow of ice through steep rugged terrain and where feedbacks with
335 often extreme topography and complex orographic meteorology are poorly documented. The
336 rate of regional glacier change in High Mountain Asia may also be enhanced when compared

337 to lower-altitude glacierised regions, as Northern Hemisphere warming is enhanced at
338 altitudes above 5000 m (Xu *et al.* 2016), the elevation range where the ELAs of the many
339 large glaciers are located (Benn & Lehmkuhl, 2000). To better understand better the impact
340 of climate change on glacier mass balance, meteorological variables on a smaller spatial scale
341 than the entire region are needed.

342

343 Predictions of glacier response to future climate change can be made either by extrapolating
344 from observations of recent glacier change and present-day glacier characteristics, or by
345 applying numerical glacier–climate models. These glacier models vary widely in their level
346 of sophistication and complexity depending on the required application, but generally can
347 either extrapolate from observed trends in the relationship between glacier mass balance and
348 climate, or replicate the physical processes by which glacier change occurs and be forced by
349 changing climate conditions. Numerical modelling of glacier mass balance forced by detailed
350 simulations of mesoscale meteorology has been undertaken to better understand the
351 atmospheric controls on Zhadang Glacier in central Tibet (Mölg *et al.* 2012), but is still in
352 development for regional applications. Glacier-climate models can be used to make
353 catchment-scale and regional-scale predictions of the contribution of glacial meltwater to
354 hydrological budgets, and their contribution in the context of water supplied by precipitation
355 or groundwater flow (e.g. Lutz *et al.* 2014). However, predictions based on numerical
356 modelling must also consider the range of uncertainties associated with the data used to drive
357 models. Many of these climatic and glaciological variables, such as the relationship between
358 air temperature and ablation beneath supraglacial debris, or the subglacial conditions
359 controlling ice flow, are poorly constrained both at present and in terms of future change in
360 the Himalaya (Rowan *et al.* 2015).

361

362 Precipitation in the monsoon-influenced Eastern and Central Himalaya is predicted to
363 increase by up to 10% during the 21st Century (IPCC scenario A2; Collins *et al.* 2013).
364 Although this increase in precipitation would mean that widespread droughts are unlikely,
365 with warmer air temperatures a greater proportion of precipitation will fall as rain rather than
366 snow and will rapidly melt glacier ice (Meehl *et al.* 2007). The mass balances of the majority
367 of glaciers in High Mountain Asia are out of equilibrium with present-day climate, as is the
368 case for glaciers worldwide. A degree day model of the Eastern Himalaya based on a 20-year
369 climate record demonstrated that loss of 25% of the glacierised area could occur with only
370 1°C warming from present (Rupper *et al.* 2012). Under an extreme scenario of 2.5°C
371 warming by the end of the 21st Century, the glacierised area of Bhutan would be reduced by
372 50%, and the contribution of meltwater flux to annual hydrological budgets would become
373 negligible (Rupper *et al.* 2012). Catchment-scale hydrological modelling of the Langtang
374 catchment in Nepal, a typical high-altitude valley in the Central Himalaya, suggest a loss of

375 35–55% of the total glacierised area by 2100, with the contribution of areal loss from debris-
376 covered glaciers only 25–33% over the same period (Ragettli *et al.* 2016).

377

378 **5. Impacts on water resources with future glacier change**

379 Until 2050, if only the contribution of glaciers to the hydrological budget is considered, river
380 flows are likely to rise during the monsoon an effect called the ‘deglaciation discharge
381 dividend’ (Kaser *et al.* 2010). River flows will reach ‘peak water’ then decline as glacier
382 mass is dramatically reduced and rivers have a greater dependence on precipitation and snow
383 melt (Soncini *et al.* 2016). ‘Peak water’ in monsoon-influenced regions is predicted to occur
384 by the mid-21st Century, as identified by hydrological modelling of glacier meltwater
385 production (Lutz *et al.* 2014). In Nepal, glacier mass loss is predicted to increase downstream
386 water supplies during the first half of the 21st Century compared to 2001–2010, as the
387 additional meltwater released each year will boost river flows. Water supplies are then either
388 predicted to decline or remain stable depending on how the monsoon changes during this
389 period, as the predicted 10% decrease in meltwater runoff could be compensated by a similar
390 increase in precipitation (Ragettli *et al.* 2016). The contribution of glacier meltwater to future
391 river flows may increase slightly during the monsoon due to enhanced ice melt, but decrease
392 overall by 4% by 2050 as glacier mass rapidly declines (Soncini *et al.* 2016). Hydrological
393 modelling predicts a decline in the glacial meltwater contribution to catchment hydrological
394 budgets over the next century; by 2065 the change in mean catchment water supply is likely
395 to be –8% in the Indus, –18% in the Ganges, and –20% in the Brahmaputra (Immerzeel *et al.*
396 2010). These decreases in meltwater supply are likely to be compensated, at least partially, by
397 increasing rainfall of +25% in the Indus and Brahmaputra and +8% in the Ganges. However,
398 these projections should be treated with caution, since changes in the monsoon are currently
399 difficult to represent in predictive climate models (Immerzeel *et al.* 2010).

400

401 Short-term increases in river flow as rainfall becomes a more important constituent of the
402 hydrological budget are likely to increase the risk of regional flooding (Ragettli *et al.* 2016).
403 However, the magnitude and timing of peak flows relative to the present day are generally
404 unknown (Fig. 4). The expansion and coalescence of supraglacial melt ponds to form larger
405 supraglacial or proglacial lakes bounded by terminal and lateral moraines presents an
406 additional risk in the form of the hazard posed by potentially catastrophic glacial lake
407 outburst floods (Benn *et al.* 2012). These sudden-onset floods generally arise from the
408 breaching of an impounding moraine, and are capable of generating peak flood discharges
409 that can exceed seasonal high flow floods by over an order of magnitude (Cenderelli and
410 Wohl, 2001). Large glacial lakes may also be considered as an intermediate storage
411 component in the hydrological cascade of glacierised (and generally deglaciating) catchments
412 and effectively regulate the downstream transmission of glacial meltwater (Carrivick and

413 Tweed, 2013). An anticipated increase in the number and extent of glacial lakes as a result of
414 climate change is of concern, especially when considered in the context of the rapidly
415 expanding Asian hydropower sector, which is likely to become increasingly exposed to
416 climatically controlled glacial flood hazards (Schwanghart *et al.* 2016), and modified
417 hydrological regimes.

418

419 Beyond 2050, sustained glacier mass loss will result in declining water supplies and possible
420 shifting of seasonal river flows, as spring meltwater will no longer sufficiently compensate
421 for the pre-monsoon dry season (Immerzeel *et al.* 2010). River flow will decline most
422 dramatically in the Indus basin where a significant proportion of the annual hydrograph is
423 derived from glacier melt (Fig. 5) (Lutz *et al.* 2014). Future river flows will depend on
424 changes in the amount and timing of precipitation, and highly seasonal river flows are likely
425 to change their timing compared to the present day, possibly resulting in enhanced spring
426 flows (Immerzeel *et al.* 2010). Total hydrological budgets are likely to decline dramatically
427 by 2100, with extreme scenarios predicting a 26% decrease in flow predicted by 2100 for the
428 Everest region, due to glaciers losing over 50% of their volume compared to 2012–2014
429 (Soncini *et al.* 2016).

430

431 **6. Improving understanding of glacier response to climate change**

432 Whilst there are large uncertainties about the current state of and the ongoing changes
433 experienced by glaciers, conclusions can nevertheless be drawn about important controls on
434 their response to climate change to make predictions of their future state (Bolch *et al.* 2012).
435 These predictions often contain large uncertainties, due to a lack of available data with which
436 to validate models, and the suitability of existing glacier models which have often been
437 developed for application to Polar ice sheets rather than glaciers flowing through steep,
438 mountainous terrain. Many factors control the response of mountain glaciers to climate
439 change (Fig. 6), and spatial and temporal variability in these controls can be challenging to
440 represent in numerical models. Some key areas for possible future research to reduce these
441 uncertainties are described here.

442

443 ***6.1 Modification of glacier response to climate change by catchment geomorphology***

444 The dynamics and hydrology of individual glaciers are governed by characteristics such as
445 glacier aspect, size, altitude, and hypsometry, collectively known as morphometry. These
446 morphometric factors exert a significant control on the dynamics and mass balance of
447 mountain glaciers (Quincey *et al.* 2009). Moreover, the pronounced interaction between high
448 topography and atmospheric circulation systems such as the Indian summer monsoon results
449 in distinctive local mesoscale meteorological patterns (Bookhagen & Burbank 2010). This
450 interaction between the atmosphere, landscape and cryosphere can produce catchment-scale

451 variations in energy and mass balance that cause adjacent glaciers to exhibit different
452 responses to the same change in climate (e.g. Glasser *et al.* 2009). For this reason, a coupled
453 mesoscale–energy balance modeling approach represents an important advance in the
454 understanding of glacier–climate interactions in High Mountain Asia (Mölg *et al.* 2012).
455 Robust dynamic or statistical methods are needed to downscale climate model outputs to a
456 scale relevant to glacier mass balance that accounts for mountainous topography (e.g.
457 Reichert *et al.* 2002). Furthermore, these relationships may need to be reconsidered for
458 application using future climatologies (Meehl *et al.* 2007). The degree-day model
459 applications, such as that used by Rupper *et al.* (2012) are useful to predict regional
460 glaciological and hydrological changes with climate variations. However, the modification of
461 glacier–climate relationships by factors such as surface debris cover and glacier morphometry
462 requires further exploration and the acquisition of field data for model validation.

463

464 ***6.2 Sensitivity of debris-covered glaciers to climate change***

465 As glaciers lose mass, debris accumulates on their surfaces, and as a result, the debris-
466 covered glacierised area worldwide is increasing. Ablation under a supraglacial debris layer
467 is primarily controlled by its thickness, but to a lesser extent by debris properties including
468 lithology, moisture content and porosity (Benn *et al.* 2012). These parameters are spatially
469 and temporally variable, due to variations in input, transport and exhumation of debris to the
470 glacier surface in space and time (Anderson & Anderson, 2016; Gibson *et al.* 2017). Much
471 recent work has focused on determining spatial variability in debris thickness, either remotely
472 using thermal satellite imagery (e.g. Mihalcea *et al.* 2008; Foster *et al.* 2012; Rounce &
473 McKinney, 2014) or directly using ground-penetrating radar (e.g. McCarthy *et al.* 2017) and,
474 in some cases, the impact of this spatial variation on glacial hydrology (Minora *et al.* 2015;
475 Soncini *et al.* 2016). Many of these inputs are validated with minimal field measurements of
476 debris thickness, but such validation would greatly extent the scope of predictions that could
477 be made considering debris-covered glacier change. Few studies currently consider the
478 influence of spatial variation in moisture content (e.g. Collier *et al.* 2014), porosity (e.g. Evatt
479 *et al.* 2015), albedo (e.g. Nicholson & Benn, 2013) or aerodynamic roughness length (e.g.
480 Rounce *et al.* 2015; Miles *et al.* 2017; Quincey *et al.* 2017).

481

482 Predictions of glacier mass balance modified by debris cover requires distributed surface
483 energy balance models that consider variations in debris cover across the glacier surface and
484 through time, and ideally simulate the interaction of free air and moisture with the porosity of
485 debris layers (e.g. Evatt *et al.* 2015, Collier *et al.* 2014). However, suitable models are few,
486 often only consider one important variable (e.g. debris thickness or porosity), and are mainly
487 driven by empirical relationships derived from limited field data (e.g. Mihalcea *et al.* 2008).
488 Therefore, to comprehensively understand the influence of a debris layer on ablation, further

489 field data is needed to quantify the extent of variations in debris parameters and to develop
490 understanding of heat flux through supraglacial debris. It is potentially possible to use field
491 measurements of debris thickness to calibrate and validate a method of classification of this
492 variable from remote observations, which would greatly extent the scope of predictions that
493 could be made considering debris-covered glacier change. Furthermore, as field-based
494 research tends to focus on relatively accessible, often smaller lower altitude glaciers, a remote
495 calibration method for debris thickness has the potential to dramatically advance knowledge
496 of how these glaciers behave in response to climatic forcing.

497

498 **6.3 Modification of glacier response to climate by glacier dynamics**

499 Feedbacks between glacier mass balance and dynamics control the magnitude and timing of
500 the response of individual glaciers to climate change. Ice flow also drives processes that
501 affect glacier mass. For example, the transport of debris to the glacier surface from englacial
502 or subglacial storage can cause the supraglacial debris layer to thicken and thereby reduce
503 ablation. In contrast, ice flow stagnation may promote the development and expansion of
504 supraglacial or moraine-dammed lakes, which promotes widespread calving of the lake-
505 terminating glacier tongue and thereby accelerating mass loss (Gardelle *et al.* 2011). Debris
506 cover frequently causes glacier tongues to lose mass by surface lowering rather than terminus
507 recession, which in turn affects dynamics, since ice flow tends to stagnate with the loss of
508 driving stress (Quincey *et al.* 2009). Commonly, supraglacial or proglacial lake formation
509 coincides with this process, and once a lake crosses a threshold of depth of about 80 m deep
510 the lake-marginal glacier ice starts to calve (Quincey *et al.* 2007, Robertson *et al.* 2012) with
511 potentially dramatic consequences for glacier dynamics and mass balance. Under IPCC 21st
512 Century climate change scenarios, proglacial lakes are increasingly likely to pose a potential
513 hazard to human life through an increased risk of sudden-onset glacial lake outburst floods.
514 However, the timing and magnitude of lake formation and growth are difficult to predict.

515

516 Rates of recent proglacial lake expansion have been quantified from satellite imagery and are
517 particularly well-studied in the Khumbu Himal in the Central Himalaya (Watson *et al.* 2016)
518 and the Lunana region of Bhutan in the Eastern Himalaya (Fujita *et al.* 2008). The primary
519 process by which lakes expand appears to be via the subaerial loss of mass at the active
520 calving front rather than the ablation of subaqueous ice, including ice at the lake bottom
521 (Fujita *et al.* 2009). Controls on calving rates for glaciers terminating in freshwater rather
522 than marine settings differ, and are dominated by wave fetch and lake temperature (Sakai *et al.*
523 2009). However, prediction of future change in these variables and the impact on lake
524 development has not been investigated. Proglacial lake growth has typically accelerated with
525 rapid glacier recession since the 1960s (Bajracharya & Mool 2010), but the impact of lake
526 formation on future glacier change is poorly understood. Although it seems intuitive that

527 lake-terminating glaciers should recede more rapidly than equivalent land-terminating
528 glaciers, few conclusive data are yet available to confirm this (e.g. King *et al.* 2017).

529

530 **7. Conclusions**

531 Glaciers in High Mountain Asia are changing rapidly in response to recent climate change,
532 with many glaciers losing mass at accelerated rates since the 1990s. Sustained glacier mass
533 loss is predicted to continue through the 21st and 22nd Centuries even in the absence of further
534 climate warming from the present day. In the monsoon-influenced Eastern and Central
535 Himalaya, the majority of glacier mass loss occurs during the warm summer months (June to
536 September), which coincides with the timing of maximum precipitation at high altitudes. As a
537 result, the glacier meltwater contribution to the Ganges and Brahmaputra catchments is
538 relatively less important than for the Indus catchment, which drains the Westerly influenced
539 Western Himalaya, Karakoram and Hindu Kush and has a smaller rainfall component of the
540 annual hydrological budget. Seasonal river flows in the Eastern and Central Himalaya are
541 therefore unlikely to decrease during the next 50 years and may even increase slightly, the
542 ‘deglaciation discharge dividend’, as climate models predict increased monsoon precipitation
543 with warming during this century, and because accelerated glacier melt will provide
544 additional water over the same period. In the Western Himalaya, Karakoram and Hindu
545 Kush, river flows are much more dependent on glacier mass change than in the catchments
546 further to the east. The future of these glaciers is a less clear, as those in the Karakoram
547 appear to have recently experienced a slightly increase in ice mass which may be due to the
548 increased extent of winter snowfall resulting from warming air temperatures. However, in the
549 Western Himalaya, glacier mass loss appears similar to that elsewhere in the mountain range,
550 suggesting that the hydrological budget of the Indus is likely to be severely affected by
551 climate change.

552

553 Beyond the mid-21st Century, when large volumes of glacier ice have been lost, the
554 hydrological budget of catchments in the monsoon-influenced regions will be more
555 dependent on the timing and availability of monsoon precipitation than glacier melt.
556 Therefore, water availability is unlikely to decrease in the short term, as a warming climate
557 will result in decreasing glacier runoff compensated by increased monsoon precipitation, with
558 little change in the seasonality of river flows. In the Westerly influenced regions, glacier
559 mass loss will likely lead to decreased river flows, and although glaciers in the Karakoram
560 are at present showing slightly positive mass balances, this trend is unlikely to continue with
561 sustained climate warming in the longer-term. As rainfall becomes a more important
562 component of the total hydrological budget, the risk of flooding is predicted to increase as
563 rainfall is transferred much more rapidly into rivers than snow that accumulates as glacier ice.
564 In the longer term, by the start of the 22nd Century, the predicted loss of over 50% of glacier

565 volume and the complete removal of smaller, lower-altitude glaciers across High Mountain
566 Asia is likely to result in a widespread decline in water supplies, which will have a dramatic
567 impact on the large populations relying on these glacier-fed rivers.

568

569 **Acknowledgements**

570 We thank Tobias Bolch and Arthur Lutz for sharing regional and catchment boundaries and
571 model outputs used to draw the figures.

572

573

574 **Figure captions**

575 Figure 1. High Mountain Asia, showing the Himalaya, Karakoram and Hindu Kush regions
576 defined by Bolch *et al.* (2012) and major rivers. The location of glaciers for which
577 glaciological mass balance records exist and the length of the record in years (Bolch *et al.*
578 2012; Pratap *et al.* 2016; Soncini *et al.* 2016; Tshering & Fujita 2016), and Vincent *et al.*
579 (2016), and the location of automatic weather stations (AWS) collecting data at high altitudes
580 are also indicated. The names of individual glaciers or glacierised regions referred to in the
581 text are highlighted in bold.

582

583 Figure 2. The surface features of Khumbu Glacier in the Everest region of Nepal, showing (a)
584 the debris-covered ablation area, looking to the south, (b) the Khumbu Icefall marking the
585 transition between the clean-ice accumulation area and the debris-covered ablation area, (c
586 and d) typical ice cliffs and supraglacial ponds in the ablation area showing englacial debris
587 layers within the ice, likely resulting from ice-rock avalanching (note figures circled in red
588 for scale).

589

590 Figure 3. Direct measurements of mass balance for six glaciers in the Himalaya between
591 1992 and 2012, showing; (a) annual mass balance, (b) cumulative annual mass balance, and
592 (c) cumulative mass balance normalised by glacier terminus altitude. Note that the data for
593 Kangwure Glacier between 1994 and 2008 (dashed line) are reconstructed mass balance
594 values derived from meteorological data using the relationship between *in situ* mass balance
595 measurements made in other years. Redrawn from Yao *et al.* (2012). See Figure 1 for the
596 locations of these glaciers.

597

598 Figure 4. Schematic diagram showing hypothetical changes in glacier volume and meltwater
599 release from mountain glaciers in response to regional climate warming over a period
600 equivalent to their last advance and recession, from the Little Ice Age maximum through the
601 present day and 21st Century.

602

603 Figure 5. Annual hydrographs for headwaters of the major Himalayan catchments produced
604 using a hydrological model for a present-day reference period of 1998–2007, showing the
605 contribution to the total hydrological budget from glacier melt, snow melt, rainfall–runoff
606 and base (groundwater) flow [redrawn from Lutz *et al.* (2014)], for (a) the Indus in the
607 westerly influenced Western Himalaya, (b) the Ganges in the transition between the westerly
608 and monsoon-influenced Central Himalaya, and (c) the Brahmaputra in the monsoon-
609 influenced Central and Eastern Himalaya. (d) shows the catchment boundaries used to make
610 these calculations, with topographic imagery from Google OpenLayers.

611

612 Figure 6. Climatic, glaciological and landscape space–time controls on glacier and climate
613 change in the Himalaya and Karakoram.

614

615

616

617

618 **References**

- 619 Adhikari, S. & Huybrechts, P. 2009. Numerical modelling of historical front
620 variations and the 21st-century evolution of glacier AX010, Nepal Himalaya. *Annals*
621 *of Glaciology*, **50**, 27–34.
- 622 Anderson, L.S. & Anderson, R.S., 2016. Modeling debris-covered glaciers: response
623 to steady debris deposition. *The Cryosphere*, **10**, 1105–1124.
- 624 Arendt, A., A. Bliss, T. Bolch, J.G. Cogley, A.S. Gardner, J.-O. Hagen, R. Hock, M.
625 Huss, G. Kaser, C. Kienholz, W.T. Pfeffer, G. Moholdt, F. Paul, V. & Radić, *et al.*,
626 2015, Randolph Glacier Inventory – A Dataset of Global Glacier Outlines: Version
627 5.0. Global Land Ice Measurements from Space, Boulder Colorado, USA. Digital
628 Media.
- 629 Azam, M.F., Wagnon, P., Ramanathan, A., Vincent, C., Sharma, P., Arnaud, Y.,
630 Linda, A., Pottakkal, J.G., Chevallier, P., Singh, V.B. & Berthier, E., 2012. From
631 balance to imbalance: a shift in the dynamic behaviour of Chhota Shigri glacier,
632 western Himalaya, India. *Journal of Glaciology*, **58**, 315-324.
- 633 Bajracharya, S.R. & Mool, P. 2010. Glaciers, glacial lakes and glacial lake outburst
634 floods in the Mount Everest region, Nepal. *Annals of Glaciology*, **50**, 81–86.
- 635 Benn, D.I. & Lehmkuhl, F. 2000. Mass balance and equilibrium-line altitudes of
636 glaciers in high-mountain environments. *Quaternary International*, **65**, 15–29.
- 637 Benn, D.I., Owen, L.A., Osmaston, H.A., Seltzer, G.O., Porter, S.C. & Mark, B.
638 2005. Reconstruction of equilibrium-line altitudes for tropical and sub-tropical
639 glaciers. *Quaternary International*, **138**, 8–21.

640 Benn, D.I., Bolch, T., Hands, K., Gulley, J., Luckman, A., Nicholson, L.I., Quincey,
641 D., Thompson, S., Toumi, R. & Wiseman, S., 2012. Response of debris-covered
642 glaciers in the Mount Everest region to recent warming, and implications for outburst
643 flood hazards. *Earth Science Reviews*, **114**, 156–174.

644 Berthier, E., Vincent, C., Magnússon, E., Gunnlaugsson, Á.P., Pitte, P., Le Meur, E.,
645 Masiokas, M., Ruiz, L., Pálsson, F., Belart, J.M.C. & Wagnon, P., 2014. Glacier
646 topography and elevation changes derived from Pléiades sub-meter stereo images.
647 *The Cryosphere*, **8**, 2275–2291.

648 Bolch, T., Pieczonka, T. & Benn, D.I. 2011. Multi-decadal mass loss of glaciers in
649 the Everest area (Nepal Himalaya) derived from stereo imagery. *The Cryosphere*, **5**,
650 349–358.

651 Bolch, T., Kulkarni, A., Kääb, A., Huggel, C., Paul, F., Cogley, J.G., Frey, H.,
652 Kargel, J.S., Fujita, K., Scheel, M. & Bajracharya, S., 2012. The state and fate of
653 Himalayan glaciers. *Science*, **336**, 310-314.

654 Bookhagen, B. & Burbank, D. 2010. Towards a complete Himalayan hydrologic
655 budget: The spatiotemporal distribution of snow melt and rainfall and their impact on
656 river discharge. *Journal of Geophysical Research*, **115**, F03019.

657 Brun, F., Buri, P., Miles, E.S., Wagnon, P., Steiner, J., Berthier, E., Ragetti, S.,
658 Kraaijenbrink, P., Immerzeel, W.W. & Pellicciotti, F. 2016. Quantifying volume loss
659 from ice cliffs on debris-covered glaciers using high-resolution terrestrial and aerial
660 photogrammetry. *Journal of Glaciology*, 1–12.

661 Brun, F., Berthier, E., Wagnon, P., Kääb, A. & Treichler, D. 2017. A spatially
662 resolved estimate of High Mountain Asia glacier mass balances from 2000 to 2016,
663 *Nature Geoscience*, **482**, 514–7.

664 Buri, P., Miles, E.S., Steiner, J.F., Immerzeel, W.W., Wagnon, P. & Pellicciotti, F.
665 2016. A physically based 3 - D model of ice cliff evolution over debris-covered
666 glaciers. *Journal of Geophysical Research: Earth Surface*, **121**, 2471–2493.

667 Carrivick, J.L. & Tweed, F.S. 2013. Proglacial lakes: character, behaviour and
668 geological importance. *Quaternary Science Reviews*, **78**, 34-52.

669 Cenderelli, D.A. & Wohl, E.E. 2001. Peak discharge estimates of glacial-lake
670 outburst floods and "normal" climatic floods in the Mount Everest region, Nepal.
671 *Geomorphology*, **1**, 57-90.

672 Cogley, J.G. 2011. Himalayan Glaciers in 2010 and 2035. In: Singh, V. P., Singh, P.
673 & Haritashya, U. (Eds.) *Encyclopedia of Snow, Ice and Glaciers*. Springer,
674 Dordrecht.

675 Collier, E., Nicholson, L.I., Brock, B.W., Maussion, F., Essery, R. & Bush, A.B.G.
676 2014. Representing moisture fluxes and phase changes in glacier debris cover using a
677 reservoir approach. *The Cryosphere*, **8**, 1429–1444.

678 Collins, M., Knutti, R. & Arblaster, J. 2013. Long-term Climate Change: Projections,
679 Commitments and Irreversibility. In: Climate Change 2013: The Physical Science
680 Basis. Contribution of Working Group I to the Fifth Assessment Report of the
681 Intergovernmental Panel on Climate Change [Stocker, T.F., D. Qin, G.-K. Plattner,
682 M. Tignor, S.K. Allen, J. Boschung, A. Nauels, Y. Xia, V. Bex and P.M. Midgley
683 (Eds.)]. Cambridge University Press, Cambridge, 1–108.

684 Evatt, G.W., Abrahams, I.D., Heil, M. & Mayer, C. 2015. Glacial melt under a
685 porous debris layer. *Journal of Glaciology*, **61**, 825–836.

686 Foster, L.A. Brock, B.W., Cutler, M.E.J. & Diotri, 2012. A physically based method
687 for estimating supraglacial debris thickness from thermal band remote-sensing data.
688 *Journal of Glaciology*, **58**, 677–691.

689 Frey, H., Machguth, H., Huss, M., Huggel, C., Bajracharya, S., Bolch, T., Kulkarni,
690 A., Linsbauer, A., Salzmann, N. & Stoffel, M. 2014. Estimating the volume of
691 glaciers in the Himalaya–Karakoram region using different methods, *The*
692 *Cryosphere*, **8**, 2313–2333.

693 Fujita, K. & Nuimura, T. 2011. Spatially heterogeneous wastage of Himalayan
694 glaciers. *Proceedings of the National Academy of Sciences*, **108**, 14011–14014.

695 Fujita, K., Suzuki, R., Nuimura, T. & Sakai, A. 2008. Performance of ASTER and
696 SRTM DEMs, and their potential for assessing glacial lakes in the Lunana region,
697 Bhutan Himalaya. *Journal of Glaciology*, **54**, 220–228.

698 Fujita, K., Sakai, A., Nuimura, T., Yamaguchi, S. & Sharma, R.R. 2009. Recent
699 changes in Imja Glacial Lake and its damming moraine in the Nepal Himalaya
700 revealed by *in situ* surveys and multi-temporal ASTER imagery. *Environmental*
701 *Research Letters*, **4**, 045205.

702 Gades, A., Conway, H., Nereson, N., Naito, N. & Kadota, T. 2000. Radio echo-
703 sounding through supraglacial debris on Lirung and Khumbu Glaciers, Nepal
704 Himalayas. *Publications of the International Association of Hydrological Sciences*,
705 **264**, 13–24.

706 Gardner, A.S., Moholdt, G., Cogley, J.G., Wouters, B., Arendt, A.A., Wahr, J.,
707 Berthier, E., Hock, R., Pfeffer, W.T., Kaser, G. & Ligtenberg, S.R., 2013. A
708 reconciled estimate of glacier contributions to sea level rise: 2003 to 2009. *Science*,
709 **340**, 852-857.

710 Gardelle, J., Arnaud, Y. & Berthier, E., 2011. Contrasted evolution of glacial lakes
711 along the Hindu Kush Himalaya mountain range between 1990 and 2009. *Global and*
712 *Planetary Change*, **75**, 47-55.

713 Gardelle, J., Berthier, E. & Arnaud, Y. 2012. Slight mass gain of Karakoram glaciers
714 in the early twenty-first century. *Nature Geoscience*, **5**, 322-325.

715 Gibson, M. J., Glasser, N. F., Quincey, D. J., Mayer, C., Rowan, A. V. & Irvine-
716 Fynn, T. D. L. 2017. Temporal variations in supraglacial debris distribution on
717 Baltoro Glacier, Karakoram between 2001 and 2012. *Geomorphology*, **295**, 572–585.

718 Glasser, N.F., Harrison, S. & Jansson, K.N. 2009. Topographic controls on glacier
719 sediment-landform associations around the temperate North Patagonian Icefield.
720 *Quaternary Science Reviews*, **28**, 2817–2832.

721 Grove, J.M. 2004. *The Little Ice Age: Ancient and Modern*, 2nd Ed. Routledge.

722 Hambrey, M.J., Quincey, D.J., Glasser, N.F., Reynolds, J.M., Richardson, S.J. &
723 Clemmens, S. 2008. Sedimentological, geomorphological and dynamic context of
724 debris-mantled glaciers, Mount Everest (Sagarmatha) region, Nepal. *Quaternary
725 Science Reviews*, **27**, 2361–2389.

726 Harper, J. & Humphrey, N. 2003. High altitude Himalayan climate inferred from
727 glacial ice flux. *Geophysical Research Letters*, **30**, 1764.

728 Hou, S., Qin, D., Yao, T., Zhang, D. & Chen, T. 2002. Recent change of the ice core
729 accumulation rates on the Qinghai-Tibetan Plateau. *Chinese Science Bulletin*, **47**,
730 1746–1749.

731 Immerzeel, W.W., van Beek, L.P.H. & Bierkens, M.F.P. 2010. Climate Change Will
732 Affect the Asian Water Towers. *Science*, **328**, 1382–1385.

733 Kadota, T., Fujita, K., Seko, K., Kayastha, R.B. & Ageta, Y. 1997. Monitoring and
734 prediction of shrinkage of a small glacier in the Nepal Himalaya. *Annals of
735 Glaciology*, **24**, 90–94.

736 Kapnick, S.B., Delworth, T.L., Ashfaq, M., Malyshev, S. & Milly, P.C.D., 2014.
737 Snowfall less sensitive to warming in Karakoram than in Himalayas due to a unique
738 seasonal cycle. *Nature Geoscience*, **7**, 834–840.

739 Kaser, G., Großhauser, M. & Marzeion, B. 2010. Contribution potential of glaciers to
740 water availability in different climate regimes. *Proceedings of the National Academy
741 of Sciences*, **107**, 20223–20227.

742 Kayastha, R.B. & Harrison, S.P. 2008. Changes of the equilibrium-line altitude since
743 the Little Ice Age in the Nepalese Himalaya. *Annals of Glaciology*, **48**, 93–99.

744 Kääb, A., Berthier, E., Nuth, C., Gardelle, J. & Arnaud, Y. 2012. Contrasting patterns
745 of early twenty-first-century glacier mass change in the Himalayas. *Nature*, **488**,
746 495–498.

747 King, O., Quincey, D.J. Carrivick, J.L. & Rowan, A.V. 2017. Spatial variability in
748 mass loss of glaciers in the Everest region, central Himalayas, between 2000 and
749 2015. *The Cryosphere*, **11**, 407–426.

750 Lutz, A.F., Immerzeel, W.W., Shrestha, A.B. & Bierkens, M.F.P. 2014. Consistent
751 increase in High Asia's runoff due to increasing glacier melt and precipitation. *Nature
752 Climate Change*, **4**, 587–592.

753 McCarthy, M., Pritchard, H., Willis, I. & King, E. 2017. Ground-penetrating radar
754 measurements of debris thickness on Lirung Glacier, Nepal. *Journal of Glaciology*,
755 **63**, 543–555.

756 Meehl, G., Stocker, T. & Collins, W.D. 2007. Global Climate Projections. In:
757 Climate Change 2007: The Physical Science Basis. Contribution of Working Group I
758 to the Fourth Assessment Report of the Intergovernmental Panel on Climate Change
759 [Solomon, S., D. Qin, M. Manning, Z. Chen, M. Marquis, K.B. Averyt, M. Tignor
760 and H.L. Miller (Eds.)]. Cambridge University Press, Cambridge, United Kingdom
761 and New York, NY, USA.

762 Mihalcea, C., Mayer, C., Diolaiuti, G., D'Agata, C., Smiraglia, C., Lambrecht, A.,
763 Vuillermoz, E. & Tartari, G., 2008. Spatial distribution of debris thickness and
764 melting from remote-sensing and meteorological data, at debris-covered Baltoro
765 glacier, Karakoram, *Annals of Glaciology*, **48**, 49-57.

766 Miles, E.S., Pellicciotti, F., Willis, I.C., Steiner, J.F., Buri, P. & Arnold, N.S. 2016.
767 Refined energy-balance modelling of a supraglacial pond, Langtang Khola, Nepal.
768 *Annals of Glaciology*, **57**, 29–40.

769 Miles, E. S., Steiner, J. F., & Brun, F. 2017. Highly variable aerodynamic roughness
770 length (z_0) for a hummocky debris-covered glacier. *Journal of Geophysical*
771 *Research: Atmospheres*, 1–58.

772 Minora, U., Senese, A., Bocchiola, D., Soncini, A., D'agata, C., Ambrosini, R.,
773 Mayer, C., Lambrecht, A., Vuillermoz, E., Smiraglia, C. & Diolaiuti, G., 2015. A
774 simple model to evaluate ice melt over the ablation area of glaciers in the Central
775 Karakoram National Park, Pakistan. *Annals of Glaciology*, **48**, 49–57.

776 Mölg, T., Maussion, F., Yang, W. & Scherer, D. 2012. The footprint of Asian
777 monsoon dynamics in the mass and energy balance of a Tibetan glacier. *The*
778 *Cryosphere*, **6**, 1445–1461.

779 Muller, F. 1961. Khumbu moraine series, Nepal. *Radiocarbon*, **3**, 16.

780 Murari, M.K., Owen, L.A., Dortch, J.M., Caffee, M.W., Dietsch, C., Fuchs, M.,
781 Haneberg, W.C., Sharma, M.C. & Townsend-Small, A., 2014. Timing and climatic
782 drivers for glaciation across monsoon-influenced regions of the Himalayan–Tibetan
783 orogen. *Quaternary Science Reviews*, **88**, 159-182.

784 Nakawo, M., Ybuki, H. & Sakai, A. 1999. Characteristics of Khumbu Glaciers,
785 Nepal Himalaya: recent change in the debris-covered area. *Annals of Glaciology*, **28**,
786 118–122.

787 Nicholson, L. & Benn, D. 2006. Calculating ice melt beneath a debris layer using
788 meteorological data. *Journal of Glaciology*, **52**, 463–470.

789 Nicholson, L. & Benn, D.I. 2013. Properties of natural supraglacial debris in relation
790 to modelling sub-debris ice ablation. *Earth Surface Processes and Landforms*, **38**,
791 490-501.

792 Østrem, G. 1959. Ice melting under a thin layer of moraine, and the existence of ice
793 cores in moraine ridges. *Geografiska Annaler*, **41**, 228–230.

794 Owen, L.A. 2009. Latest Pleistocene and Holocene glacier fluctuations in the
795 Himalaya and Tibet. *Quaternary Science Reviews*, **28**, 2150–2164.

796 Owen, L.A. & Benn, D.I. 2005. Equilibrium-line altitudes of the Last Glacial
797 Maximum for the Himalaya and Tibet: an assessment and evaluation of results.
798 *Quaternary International*, **138**, 55–78.

799 Owen, L., Caffee, M. & Finkel, R. 2008. Quaternary glaciation of the Himalayan–
800 Tibetan orogen. *Journal of Quaternary Science*, **23**, 513–531.

801 Owen, L.A., Robinson, R., Benn, D.I., Finkel, R.C., Davis, N.K., Yi, C., Putkonen,
802 J., Li, D. & Murray, A.S., 2009. Quaternary glaciation of Mount Everest. *Quaternary
803 Science Reviews*, **28**, 1412–1433.

804 Owen, L.A. & Dortch, J.M. 2014. Quaternary Science Reviews. *Quaternary Science
805 Reviews*, **88**, 14–54.

806 Pratap, B., Dobhal, DP, Mehta, M & Bhambri, R 2015. Influence of debris cover and
807 altitude on glacier surface melting: a case study on Dokriani Glacier, central
808 Himalaya, India. *Annals of Glaciology*, **56**, 9–16.

809 Pritchard, H.D. 2017. Asia’s glaciers are a regionally important buffer against
810 drought. *Nature*, **545**, 169–174.

811 Quincey, D.J., Richardson, S.D., Luckman, A., Lucas, R.M., Reynolds, J.M.,
812 Hambrey, M.J. & Glasser, N.F., 2007. Early recognition of glacial lake hazards in the
813 Himalaya using remote sensing datasets. *Global and Planetary Change*, **56**, 137-152.

814 Quincey, D.J., Luckman, A. & Benn, D. 2009. Quantification of Everest region
815 glacier velocities between 1992 and 2002, using satellite radar interferometry and
816 feature tracking. *Journal of Glaciology*, **55**, 596–606.

817 Quincey, D.J., Braun, M., Glasser, N.F., Bishop, M.P., Hewitt, K. & Luckman, A.
818 2011. Karakoram glacier surge dynamics. *Geophysical Research Letters*, **38**.

819 Quincey, D.J., Glasser, N.F., Cook, S.J. & Luckman, A. 2015. Heterogeneity in
820 Karakoram glacier surges. *Journal of Geophysical Research: Earth Surface*, **120**,
821 1288-1300.

822 Quincey, D., Smith, M., Rounce, D., Ross, A., King, O., & Watson, C.S. 2017.
823 Evaluating morphological estimates of the aerodynamic roughness of debris covered
824 glacier ice. *Earth Surface Processes and Landforms*, **49**, 547–44.

825 Ragettli, S., Immerzeel, W.W. & Pellicciotti, F. 2016. Contrasting climate change
826 impact on river flows from high-altitude catchments in the Himalayan and Andes
827 Mountains. *Proceedings of the National Academy of Sciences*, **113**, 9222-9227.

828 Reichert, B.K., Bengtsson, L. & Oerlemans, J. 2002. Recent glacier retreat exceeds
829 internal variability. *Journal of Climate*, **15**, 3069–3081.

830 Reid, T.D. & Brock, B.W. 2014. Assessing ice-cliff backwasting and its contribution
831 to total ablation of debris-covered Miage glacier, Mont Blanc massif, Italy. *Journal*
832 *of Glaciology*, **60**, 3–13.

833 Reznichenko, N., Davies, T. & Shulmeister, J. 2010. Effects of debris on ice-surface
834 melting rates: an experimental study. *Journal of Glaciology*, **56**, 384–394.

835 Robertson, C.M., Benn, D.I., Brook, M.S., Fuller, I.C. & Holt, K.A. 2012.
836 Subaqueous calving margin morphology at Mueller, Hooker and Tasman glaciers in
837 Aoraki/Mount Cook National Park, New Zealand. *Journal of Glaciology*, **58**, 1037–
838 1046.

839 Rounce, D.R., Quincey, D.J. & McKinney, D.C. 2015. Debris-covered glacier energy
840 balance model for Imja–Lhotse Shar Glacier in the Everest region of Nepal. *The*
841 *Cryosphere*, **9**, 2295–2310.

842 Rowan, A.V. 2017. The 'Little Ice Age' in the Himalaya: A review of glacier advance
843 driven by Northern Hemisphere temperature change. *The Holocene*, **27**, 292–308.

844 Rowan, A.V., Egholm, D.L., Quincey, D.J. & Glasser, N.F. 2015. Modelling the
845 feedbacks between mass balance, ice flow and debris transport to predict the
846 response to climate change of debris-covered glaciers in the Himalaya. *Earth and*
847 *Planetary Science Letters*, **430**, 427–438.

848 Röthlisberger, R. F. & Geyh, M. 1986. Glacier variations in Himalayas and
849 Karakorum. *Journal of Glaciology and Geocryology*, **4**, 237–249.

850 Rupper, S., Schaefer, J.M., Burgener, L.K., Koenig, L.S., Tsering, K. & Cook, E.R.
851 2012. Sensitivity and response of Bhutanese glaciers to atmospheric warming.
852 *Geophysical Research Letters*, **39**, L19503.

853 Sakai, A., Nishimura, K., Kadota, T. & Takeuchi, N. 2009. Onset of calving at
854 supraglacial lakes on debris-covered glaciers of the Nepal Himalaya. *Journal of*
855 *Glaciology*, **55**, 909–917.

856 Sarikaya, M.A., Bishop, M.P., Shroder, J.F. & Olsenholler, J.A. 2012. Space-based
857 observations of Eastern Hindu Kush glaciers between 1976 and 2007, Afghanistan
858 and Pakistan. *Remote Sensing Letters*, **3**, 77–84.

859 Scherler, D., Bookhagen, B. & Strecker, M.R. 2011. Spatially variable response of
860 Himalayan glaciers to climate change affected by debris cover. *Nature Geoscience*, **4**,
861 156–159.

862 Schwanghart, W., Worni, R., Huggel, C., Stoffel, M. & Korup, O. 2016. Uncertainty
863 in the Himalayan energy-water nexus: estimating regional exposure to glacial lake
864 outburst floods. *Environmental Research Letters*, **11**, 074005.

865 Sharma, M.C. & Owen, L.A. 1996. Quaternary glacial history of NW Garhwal,
866 central Himalayas. *Quaternary Science Reviews*, **15**, 335–365.

867 Solomina, O.N., Bradley, R.S., Jomelli, V., Geirsdottir, A., Kaufman, D.S., Koch, J.,
868 McKay, N.P., Masiokas, M., Miller, G., Nesje, A. & Nicolussi, K., 2016. Glacier
869 fluctuations during the past 2000 years. *Quaternary Science Reviews*, **149**, 61–90.

870 Soncini, A., Bocchiola, D., Confortola, G., Minora, U., Vuillermoz, E., Salerno, F.,
871 Viviano, G., Shrestha, D., Senese, A., Smiraglia, C. & Diolaiuti, G., 2016. Future
872 hydrological regimes and glacier cover in the Everest region: The case study of the
873 upper Dudh Koshi basin. *Science of The Total Environment*, **565**, 1084–1101.

874 Tapley, B.D., Bettadpur, S., Ries, J. C., Thompson, P. F., & Watkins, M. M. 2004.
875 The gravity recovery and climate experiment: Mission overview and early results.
876 *Geophysical Research Letters*, **31**, L09607.

877 Thakuri, S., Salerno, F., Smiraglia, C., Bolch, T., D'Agata, C., Viviano, G. & Tartari,
878 G. 2014. Tracing glacier changes since the 1960s on the south slope of Mt. Everest
879 (central Southern Himalaya) using optical satellite imagery. *The Cryosphere*, **8**,
880 1297–1315.

881 Thompson, L.G., Mosley-Thompson, E., Davis, M.E., Mashiotta, T.A., Henderson,
882 K.A., Lin, P.-N. & Tandong, Y. 2006. Ice core evidence for asynchronous glaciation
883 on the Tibetan Plateau. *Quaternary International*, **154**, 3–10.

884 Thompson, S.S., Benn, D.I., Dennis, K. & Luckman, A. 2012. A rapidly growing
885 moraine-dammed glacial lake on Ngozumpa Glacier, Nepal. *Geomorphology*, **145**,
886 1–11.

887 Thompson, S., Benn, D.I., Mertes, J. & Luckman, A. 2016. Stagnation and mass loss
888 on a Himalayan debris-covered glacier: processes, patterns and rates. *Journal of*
889 *Glaciology*, **62**, 467–485.

890 Tshering, P. & Fujita, K. 2016. First in situ record of decadal glacier mass balance
891 (2003–2014) from the Bhutan Himalaya. *Annals of Glaciology*, **57**, 289–294.

892 Vaux, H.J. & Balk, D. 2012. National Research Council (US). Committee on
893 Himalayan Glaciers, Hydrology, Climate Change, and Implications for Water
894 Security, 2012. Himalayan glaciers: Climate change, water resources, and water
895 security. National Academies Press.

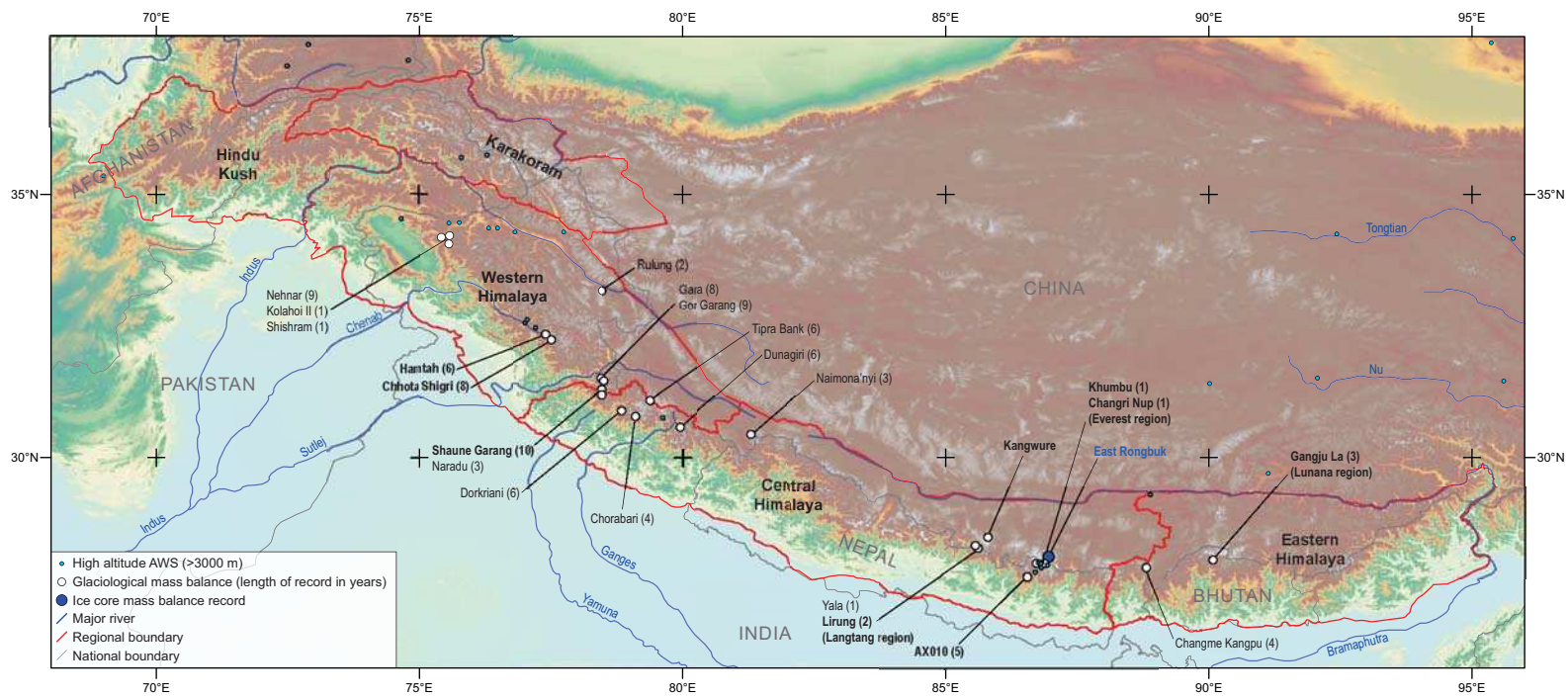
896 Vincent, C., Wagnon, P., Shea, J.M. & Immerzeel, W.W. 2016. Reduced melt on
897 debris-covered glaciers: investigations from Changri Nup Glacier, Nepal. *The*
898 *Cryosphere*, **10**, 1845–1858.

899 Watson, C.S., Quincey, D.J., Carrivick, J.L. & Smith, M.W. 2016. The dynamics of
900 supraglacial water storage in the Everest region, central Himalaya. *Global and*
901 *Planetary Change*, **142**, 14–27.

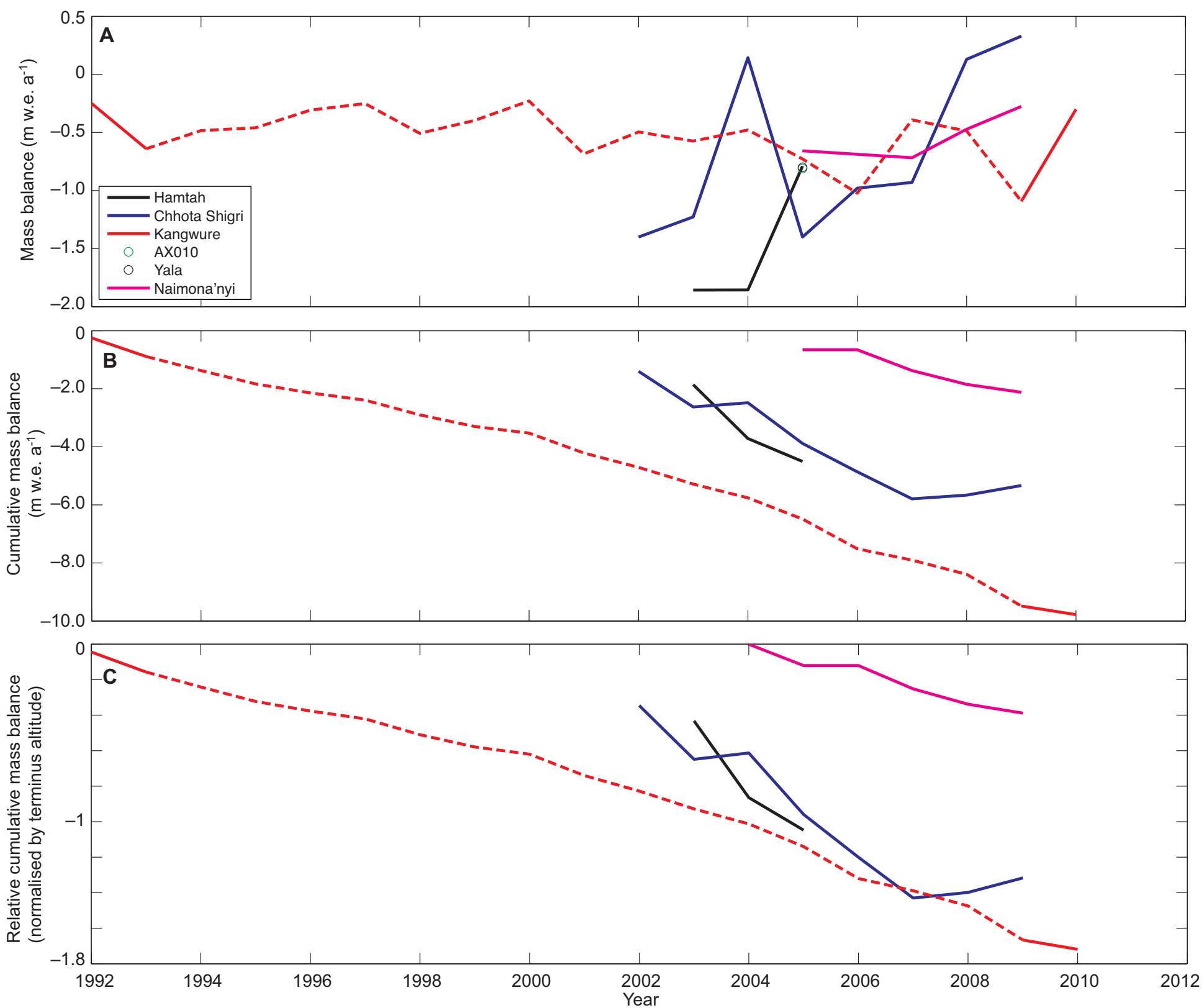
902 Xu, Y., Ramanathan, V. & Washington, W.M., 2016. Observed high-altitude
903 warming and snow cover retreat over Tibet and the Himalayas enhanced by black
904 carbon aerosols. *Atmospheric Chemistry and Physics*, **16**, 1303–1315.

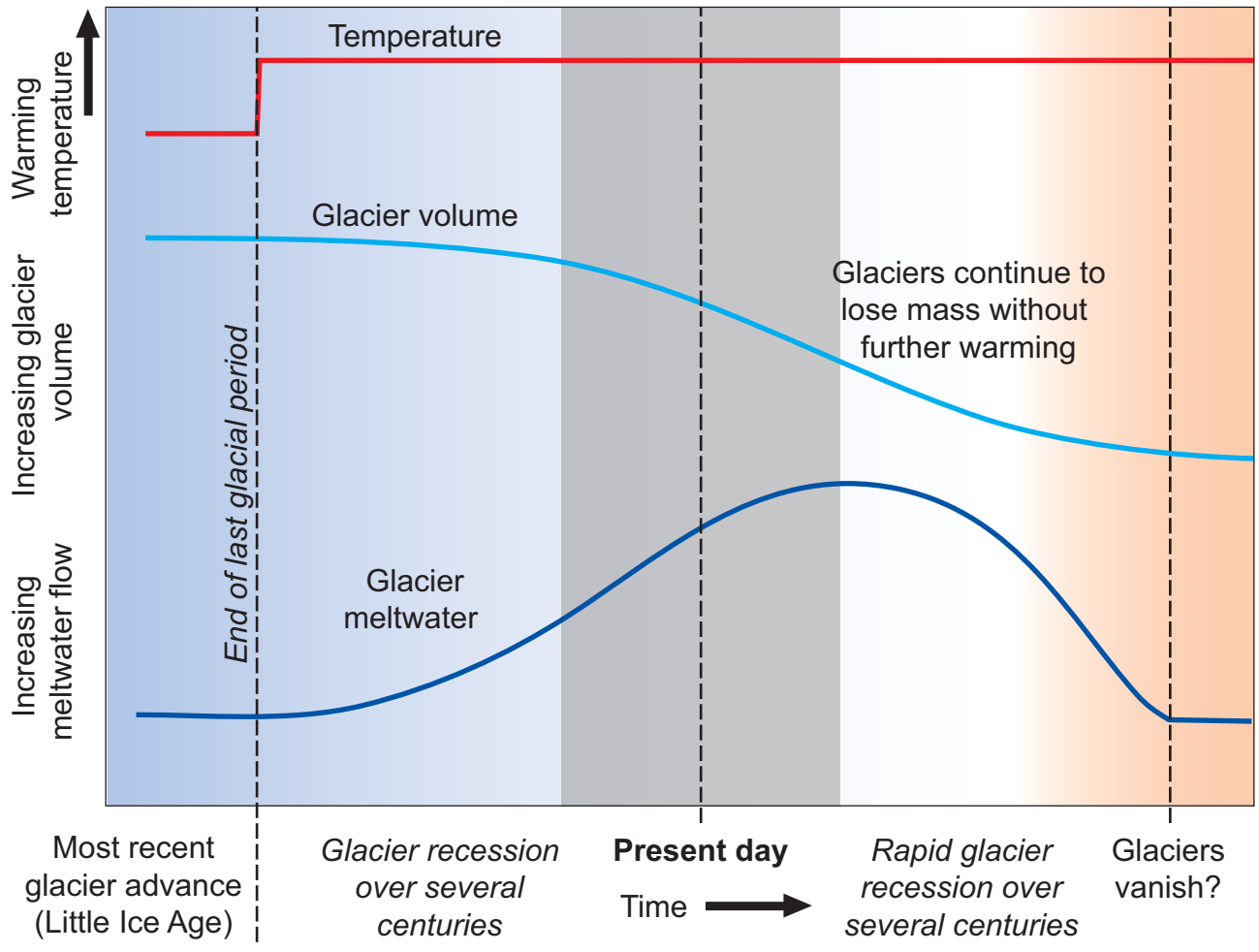
905 Yao, T., Thompson, L., Yang, W., Yu, W., Gao, Y., Guo, X., Yang, X., Duan, K.,
906 Zhao, H., Xu, B. & Pu, J., 2012. Different glacier status with atmospheric
907 circulations in Tibetan Plateau and surroundings. *Nature Climate Change*, **2**, 663-
908 667.

909









Warming temperature ↑

Increasing glacier volume

Increasing meltwater flow

Most recent glacier advance (Little Ice Age)

Glacier recession over several centuries

Present day

Time →

Rapid glacier recession over several centuries

Glaciers vanish?

End of last glacial period

Temperature

Glacier volume

Glacier meltwater

Glaciers continue to lose mass without further warming

